ZIBELINE INTERNATIONAL™ PUBLISHING

ISSN: 2521-5035 (Print)
ISSN: 2521-5043 (Online)
CODEN: ESMACU

Earth Sciences Malaysia (ESMY)

DOI: http://doi.org/10.26480/esmy.01.2022.50.55

CrossMark

RESEARCH ARTICLE

INTEGRATION OF SEISMIC REFRACTION AND LABORATORY TEST TECHNIQUES FOR SLOPE STABILITY ANALYSIS, SOUTH-SOUTH, NIGERIA

Mfoniso U. Aka[a*], Moses M. M. Ekpa[b], Christopher I. Effiong[c], Azuanamibebi D. Osu[b], Johnson C. Ibuot[d]

[a] Department of Physics, University of Uyo, Uyo, Nigeria
[b] Department of Physics, Federal College of Education (Technical), Omoku
[c] Department of Geoscience, University of Uyo, Uyo, Nigeria
[d] Department of Physics & Astronomy, University of Nigeria, Nsukka, Nigeria
****Correspondence author email: mfonisoaka@uniuyo.edu.ng***

ARTICLE DETAILS

Article History:

Received 27 May2022
Accepted 30 June 2022
Available online 07 July 2022

ABSTRACT

This study integrates seismic refraction technique (SRT) and laboratory test technique (LTT) methods in order to evaluates the slope stability characteristics of the sedimentary rocks at Mary-Slessor Secondary School, South-South, Nigeria. The integrated approach was adopted to investigate the material strength, soil resistivity and delineate optimal slopes with regards to the factor of safety (FOS). Three layers were delineated in the field analysis, the velocity and resistivity of the first, second and third layers range from (460.5 – 1050) m/s and (850 – 1220) Ωm at 5.61 m depth, (1705 – 2100) m/s, (560 – 650) Ωm at 7.20 m, and (2000 – 2500) m/s, (330 – 450) Ωm at 13.3 m respectively. The elastic parameters obtained from SRT and LTT ranged from (1.1 - 2021.1) kN/m^2 and (1.2 – 2270) kN/m^2. The result revealed the material's strengths of the third layer formation with a high velocity and low resistivity being optimally stable with regards to FOS.

KEYWORDS

Poisson ratio, Oedemetric Modulus, Compressibility, Resistivity

1. INTRODUCTION

Slope stability has become an essential factor to consider in engineering projects. It involves calculating and assessing the amount of stress a slope can manage before weakening as a result of ground movement (Gordon et al., 2016; Ray et al., 2020). A slope will likely fail whenever the driving forces (gravity) overcome the slope material's shear strength (resisting forces). According to a study, analysis of slope stability is a standard practice in geotechnical engineering, and it involves the calculation of the factor of safety (FOS) (Asteris et al., 2022). Studying slope stability enable the location of risky areas, causes of slope failures and can aid in designing of reliable slope. Through comparability of slope stableness, earth scientist and engineers established a moderate and innovational framework within the province which in the erstwhile considered hazardous for construction.

Moreover, the insight gained by determining slope stability has given subsurface geophysicists, geologists, and civil engineers, an expanded understanding of natural laws and forces, which they can study to improve future projects, as well as progress in the civil engineering and geophysical application globally, sloppy areas subjected to high loading from high-rise buildings will require higher FOS to minimize the probability of slope failure occurrence (Roc, 2005; Xiao et al., 2016). Thus, in a hilly terrain area, accessibility will be difficult for the boring technique which fetches much time, energy, and cost constraints. To lessen this menace, this current research was carried out using an integrated approach of seismic refraction with laboratory test techniques which have several advantages. Seismic refraction methods are non-destructive and more efficient with much aerial coverage data compared to laboratory borings.

Selecting the slope stability analysis method is important; however, the accuracy of the analysis relies heavily on the input data. Ideal input data requires a thorough understanding of the slope's subsurface conditions including soil types, layer thicknesses, soil strength parameters, soil unit weights, location of the water table, and relative elevations along the slope. The absence of any of these parameters decreases the accuracy and reliability of the study. However, the seismic refraction method can boost the conventional geotechnical investigation of the slope area to obtain accurate parameters needed for slope stability analysis in contrast to laboratory testing (Abudeif et al., 2017). The seismic refraction method will give information on slope layers which will be estimated based on wave velocities. That is compression wave velocity (Vp) and shear wave velocity (Vs) toward the depth of the slope area (Uhlemann et al., 2016).

According to a group researcher, analysis of slope stability is a standard practice in geotechnical engineering, and it involves the calculation of the factor of safety (FOS) (Asteris et al., 2022). Studying slope stability enables the location of risky areas and causes of slope failures and can aid in designing a reliable slope. Through comparability of slope stability, earth scientists and engineers established a moderate and innovative framework within the province which the erstwhile considered hazardous for construction. Moreover, the insight gained by determining slope stability has given subsurface geophysicists, geologists, and civil engineers, an expanded understanding of natural laws and forces, which they can study to improve future projects, as well as progress in the civil engineering and geophysical application globally, (Roc. 2005; Asteris et el., 2022).

The stability condition of slopes is a subject of study and research in soil mechanics, geotechnical engineering, and engineering geology. Slope

Quick Response Code	Access this article online	
	Website: www.earthsciencesmalaysia.com	**DOI:** 10.26480/esmy.01.2022.50.55

Cite The Article: Mfoniso U. Aka, Moses M. M. Ekpa, Christopher I. Effiong, Azuanamibebi D. Osu, Johnson C. Ibuot (2022). Integration of Seismic Refraction and Laboratory Test Techniques for Slope Stability Analysis, South-South, Nigeria. *Earth Sciences Malaysia, 6(1): 50-55.*

stability assesses the strength of earthwork, burrow, and congenital gradient in rocks (Rasouli and Mahyar, 2011). It is a measure of how resistant a natural or artificial slope is to failure due to collapse or sliding, as well as to prevent the initiation of sloppy movement, slowing it down, or arresting it through extenuation relief (Sharma et al., 2017). On the other hand, soil parameters classified as elastic, bearing, and engineering parameters can be obtained from the seismic refraction method as expressed in Eqns. 1 -7 and summarized in Table 1. Comparison will be made with the same parameters acquired from laboratory testing. In laboratory tests, rock core samples collected are used for strength tests. These include uniaxial rock tests to yield uniaxial compressive strength of soil classification and triaxial strength tests to analyze the mechanical properties of the soil parameters.

2. Location and Geology of the Study Area

The study area is Mary Slessor School terrain in Ibiono Ibom Local Government Area of Akwa Ibom State, Nigeria. It is underlain by excavated slopes, soft rock trails in reservoirs, and forests of sedimentary formation of late tertiary and Holocene ages within the tropical rainforest belts of Nigeria (Figures 1 and 2a). It is located within latitudes 5.10^{0}N – 5.15^{0}N and Longitude 7.50^{0}E – 7.55^{0}E (Aka et al., 2020). The terrain was established in 1895 by a Scottish Presbyterian Missionary; Mary Mitchell Slessor to educate Ibibio and Efik people in then Calabar axis of the Southern protectorate of Nigeria (Imbua, 2013). However, becomes a tourism center for landscape, infrastructure, architecture and cultural studies globally, as shown in Figure 2(b). It is enriched with natural resources and hydrocarbon (Akpan and Okwueze, 2006). It lies in the equatorial climatic region which experiences two seasons: wet and dry seasons between June to October and November to March respectively (Udeagha et al., 2013). Also found in the terrain are rivers, streams, and wetlands which support aquatic lives like fishes, periwinkle, shrimps, and oyster (Aka et al., 2020).

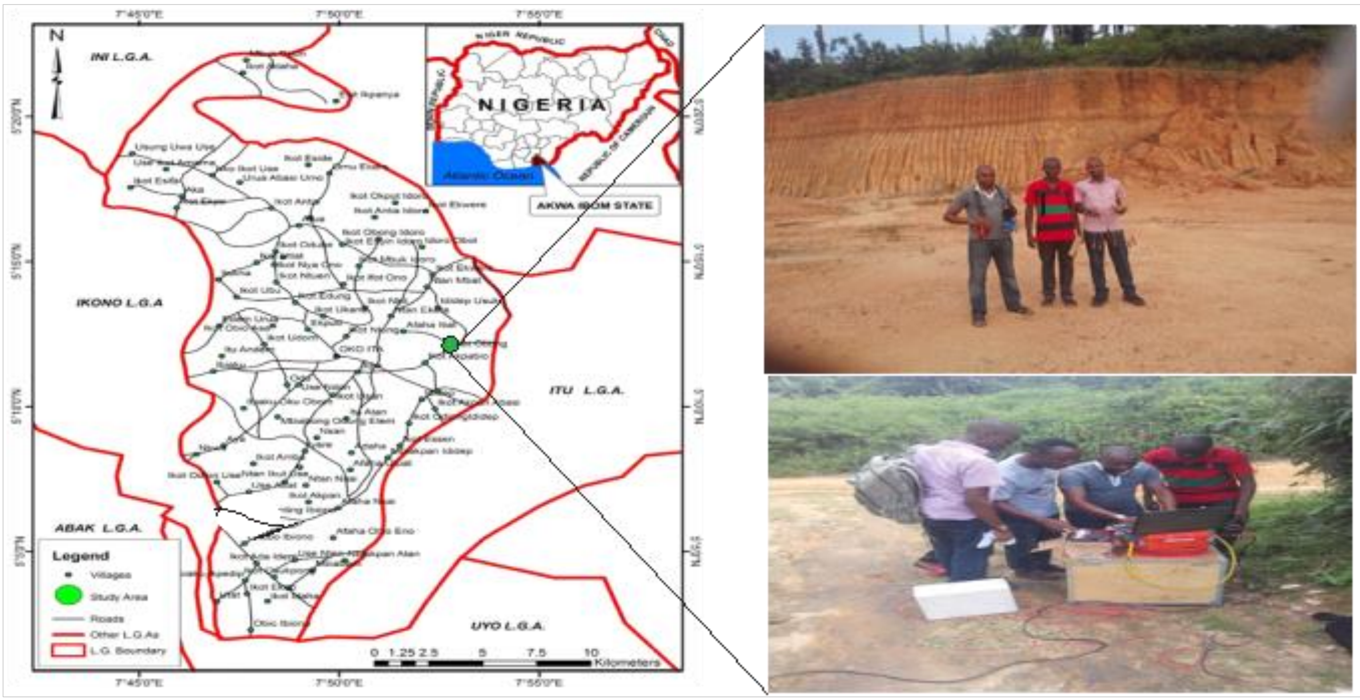

Figure 1: Map of Ibiono Ibom Showing the Study Area Terrain

Figure 2: (a) Weathered Rocks Formation (b) Statue of Mary Slessor School Terrain

2.1 Theory

The seismic refraction practice employs the concept of Snell's law to operate seismic energy which propagates through the subsurface to the top through refracted beam pathway. The seismic energy exists as Primary (P) and Secondary (S) body waves and is measured as seismic wave velocities of VP and VS. (Aka et al., 2020). These measured velocities link to the calculation of elastic and bearing properties as shown in Table 1 and Eqns. 1-7.

Table 1: Soil Parameters and their Formula

Soil Parameters	Formula
Young Modulus or Modulus of Elasticity (E)	$2\mu\,(1+\sigma)$, $\sigma = \left(\frac{\alpha-2}{2(\alpha-1)}\right)$, $\alpha = \left(\frac{V_P}{V_S}\right)^2$
Shear Modulus or Modulus of Rigidity (μ)	$\frac{\gamma {V_S}^2}{g}$ $\gamma = \gamma_o + 0.002V_P$, where $\gamma_o = 16$
Bulk Modulus or Compression Modulus (Ꝃ)	$\frac{2\mu(1+\sigma)}{3(1-2\sigma)}$
Oedometric Modulus (E_C)	$\frac{(1-\sigma)E}{(1+\sigma)(1-2\sigma)}$
Poisson Ratio or Poisson Coefficient (σ)	$\left(\frac{\alpha-2}{2(\alpha-1)}\right)$
Compressibility (β)	$\frac{1}{K}$
Compliance (C)	$\frac{1}{E}$

Modulus of Elasticity measures the rigidity of the soil materials, which relates the shear modulus "μ" and Poisson ratio "σ".

$$\text{Young Modulus or Modulus of Elasticity (E)} = 2\mu\,(1+\sigma) \quad (1)$$

Shear Modulus or modulus of rigidity (μ) measures the concurrent of elasticity for a shear force, it is expressed as the ratio of shear stress to shear strain of a solid materials.

$$\text{Shear Modulus or modulus of rigidity } (\mu) = \frac{\gamma {V_S}^2}{g} \quad (2)$$

Bulk Modulus or Compression Modulus (Ꝃ) measures the ability of a substance to withstand changes in volume under compression; it is expressed as a ratio of volumetric stress to volumetric strain of materials.

$$\text{Bulk Modulus or Compression Modulus (Ꝃ)} = \frac{2\mu(1+\sigma)}{3(1-2\sigma)} \quad (3)$$

Oedometric modulus (E_C)measures concurrent of compressibility of a materials, which relate young modulus and Poisson ratio together. (Aka et al. 2020)

$$\text{Oedometric Modulus } (E_C) = \frac{(1-\sigma)E}{(1+\sigma)(1-2\sigma)} \quad (4)$$

Poisson ratio or Poisson coefficient (σ) measures the elastic property of soil materials as a ratio of lateral strain to longitudinal strain under uniaxial loading.

$$\text{Poisson ratio or Poisson coefficient } (\sigma) = \left(\frac{\alpha-2}{2(\alpha-1)}\right) \quad (5)$$

Compressibility (β) measures the reciprocal of the bulk modulus (equation 6), which is expressed as volumetric strain to volumetric stress of a material.

$$\text{Compressibility } (\beta) = \frac{1}{K} \quad (6)$$

Compliance(C) measures the inverse of modulus of elasticity expressed as the tendency of an object to resist deformation of a material and is expressed in equation 7.

$$\text{Compliance(C)} = \frac{1}{E} \quad (7)$$

3. Method of Data Analysis

3.1 Seismic Refraction

3.1.1 Data Acquisition

In seismic refraction, the survey was carried out at 16 different locations for three-layer formations, using 24 channels ABEM 3000S enhancement seismograph. A sledgehammer of 75kg and metal plates was used as a source. S and P wave geophones of 48H_z frequency were used as detectors as shown in Figure 3(a). 120 m profile length at an inter-geophone spacing of 5 m, shot to 1st geophones separation was 5 m and total geophones of 24 per profile were used as shown in Figure 3(b). The traveling waves refracted based on the differences in soil layer before reaching the geophones. The source of elastic P and S waves was generated by blowing the sledgehammer towards the metal plates that are placed 4 mm on the ground. In P waves, 2 shots were recorded at each location with 2 stacks per shot location.

In S waves, 4 shots were recorded at each location with 2 stacks per shot location. During the blowing session of the sledgehammer to detect P and S waves, any small movement should be avoided to minimize error as geophones trigged any small walking motion. However, for geophones located close to the hammer source, the P and S waves signal will travel directly to the geophones whereas, for geophones located far away from the source, the waves will be refracted before reaching the geophones. This step has been repeated throughout the entire survey to avoid large errors in the survey results. On the other hand, other conditions that hindered the placement of geophones within the terrain include the availability of vegetation, landslides, and soil erosion.

3.1.2 Data Processing and Interpretation

Seismic refraction data acquired were processed and interpreted using Pickwin and IXrefrax software collection. Three phases were considered, the first phase elaborates on the exact picking of the first break from the seismic wave by using Pickwin software to obtain the time (T) and distance (X) of both P and S trajectories. This was grounded at outline length, geophones spacing, and its first arrival times. The second phase elaborates on the computation of P and S wave velocities from the inverted slope of T-X trajectories. The correlation of the S velocity rises with lessens in travel times owing to evolution and immersion of moisture in pores formation. However, lessening in P velocity rises as regards travel time on account of lessening in bulk modulus and soil solidity. On the other hand, the P and S velocities scheme with other parameters indicates a lineal correction allying the parameters. The third phase elaborates on the modeling of 2D near-surface parameters as shown in Figure 2. 2D modeling was preferred over 3D, to maintain the model creation complexity, simulation time, and lower costs of software purchase.

3.2 Laboratory Test Analysis

The test was performed to characterize the rock properties. The rock core samples were collected in two categories: that is, disturbed and undisturbed samples. The samples were analyzed to define the required soil parameters for slope stability analysis. The tests carried out were uniaxial rock tests to yield uniaxial compressive strength, which is a typical rock property used to correlate with the seismic velocities obtained from seismic refraction investigations. Triaxial strength tests were also performed to analyze the mechanical properties and soil classifications. The experimental index was presented as shown in Tables: 2-4. Schematically, in seismic refraction analysis, the scheme covers data acquisition, processing, and interpretation while the laboratory analyzes covers the disturbed and undisturbed samples for resistivity parameters accompanied by the geological interpretation.

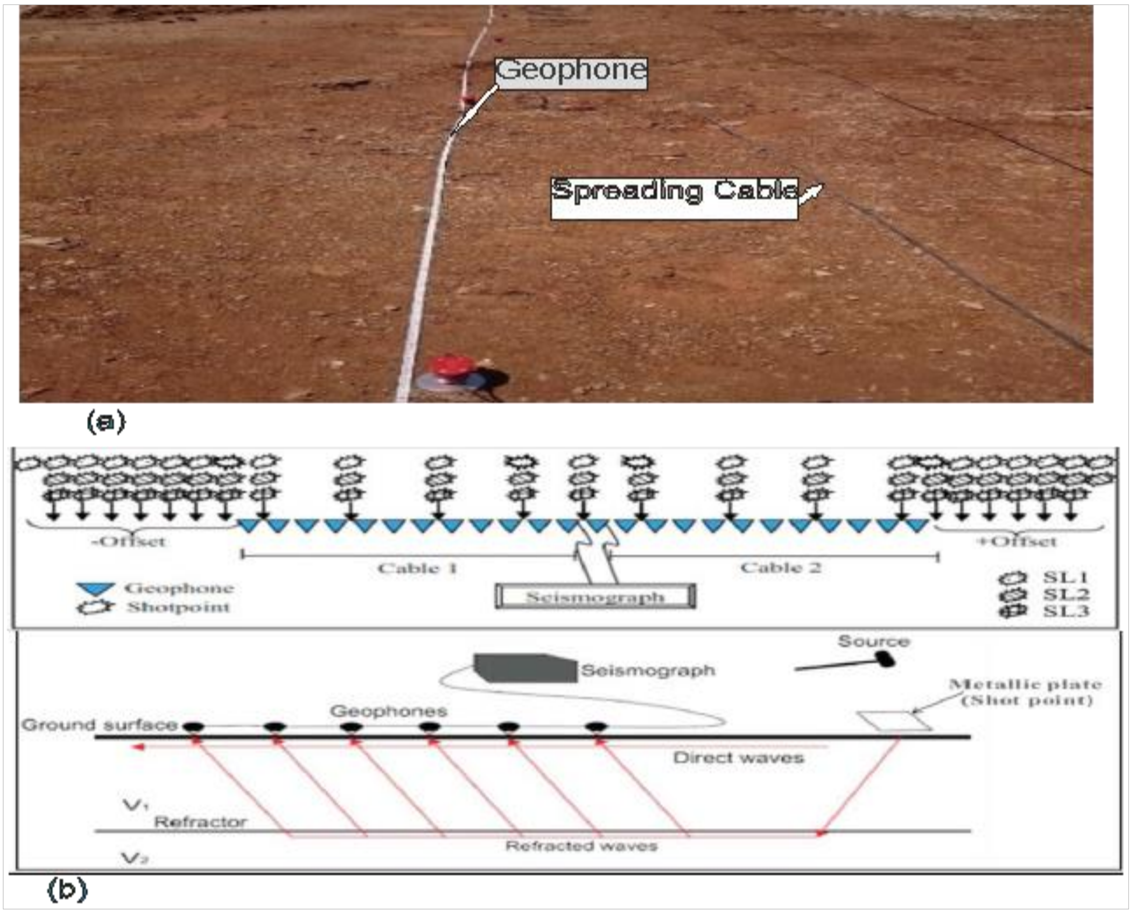

Figure 3: (a) Seismic Refraction data Acquisition layout (b) Geophone alignments

Table 2: Imaging and Geological Interpretation				
Layers	**Depth (m)**	**Colour**	**Geological Interpretations**	**Resistivity (Ωm)**
1	5.61	Red	Slate, Shale / sandy soil	850 - 1220
2	7.20	Blue	Shale / Silt	560 – 650
3	13.37	Yellow	Shale / Clayey	330 -450

Table 3: Velocity of each shot point					
Layers	**Velocities**	**Sp1**	**Sp2**	**Sp3**	**Depth (m)**
1	V_1	485.2	460.5	1050	5.61
2	V_2	1705	1900	2100	7.76
3	V_3	-	-	2500	13.32

Table 4: Soil parameters from Laboratory test and Seismic Refraction Survey			
Soil Parameters	**Laboratory Test (kN/m²)**	**Seismic Refraction Survey (kN/m²)**	**Percentage Error (%)**
Young's Modulus (E)	2270	2021.1	10.9
Shear Modulus (μ)	1202	1085.0	9.2
Bulk Modulus (κ)	310	293.6	5.3
Oedometric Modulus (E_C)	123	113.5	7.7
Compressibility (β)	40.5	34.5	14.8
Poisson Ratio	1.2	1.1	16.6

4. Result and Discussion

The seismic refraction survey with a laboratory test technique was carried out within the study area. The result from the analysis showed that the study area primarily is hidden by shale, silt and sandstone of sedimentary rock which is due to the long-term effect of weathering and deposition of mineral or organic particles of the earth's surface as shown in Table 2. Three traverses were covered, each 60 m long and inter-geophones separation of 5 m apart for 13 intervals of 12 (P and S)-wave Geophones. The shot point adopted was a linear array arrangement of geophone at three-point for each three-layer formation. Fig. 4 shows the travel time versus distance plot of two-shot point of SPI and SP3. Three portions for each of the shot point were anticipated for every point; longitude, latitude along with elevation were taken and contoured (Figure 5).

The velocity was calculated by taking the inverse of the slope value of each point such that every point gives a different velocity. Different seismic velocities and depths (Table 3) encountered due to the elasticity of soil layers which are: First layer: V^1 ranging from 485.2 – 460.5 m/s, for SP1 and SP2 showed weathered sandstone. For SP3: V^1 was 1050 m/s, and 5.61 m showing fractured granite. Second layer: V^2 ranging from 1705 - 1900 m/s, for SP1 and SP2, and 2100 m/s for SP3 and 7.76 m showing apparently fractured sandstone. Third layer V^3 range from 2000 - 2500 m/s for SP1, SP2 and SP3, and 13.32m showing hardly fractured granite. The soil parameters: Young Modulus, Shear Modulus, Bulk Modulus, Oedometric Modulus, Compressibility and Poisson ratio average values were: 2021.1, 1085.0, 293.6, 113.5, 34.5 and 1.1 kN/m³.

In laboratory testing: the uniaxial rock test, and triaxial strength test were carried out, the result from the analysis showed that the friction angle and cohesion of the respective soil samples were 44.6⁰ and 14 kN/m² respectively. The average values of the Young Modulus, Shear Modulus, Bulk Modulus, Oedometric Modulus, Compressibility and Poisson ratio were; 2270, 1202, 310, 123, 40.5 and 1.2 kN/m^2 respectively. The general classification of slope stability was established based on the soil properties obtained from seismic refraction and laboratory test methods. Thus, the comparison was made to justify their similarities as shown in Table 4. The results showed that the six soil parameters obtained from both methods were similar with percentage error ranging from 5.3 % to 16.6 % as illustrated in the histogram as shown in Figure 6.

The deformation observed in the soil parameters is due to the non-linear behavior of most soil and rock masses which depends on the occurring frequency. The frequencies in seismic waves are normally not the same as frequencies used in dynamic testing. On the other hand, shear stress and strain in seismic waves are smaller compared to stress and strain in the laboratory tests. Finally, the slope stability was delineated in terms of slope FOS which was analyzed based on the data captured from laboratory tests. These were aimed to differentiate between safe slope and slope with the elevated prospect of failure occurrence. In view of this, a safe slope was observed to have FOS of at least 1 whereas the slope with failure prospect was having FOS of less than 1. Hence, a general classification of slope stability is made on the evaluation by virtue of soil parameters and clearly slope factor of safety.

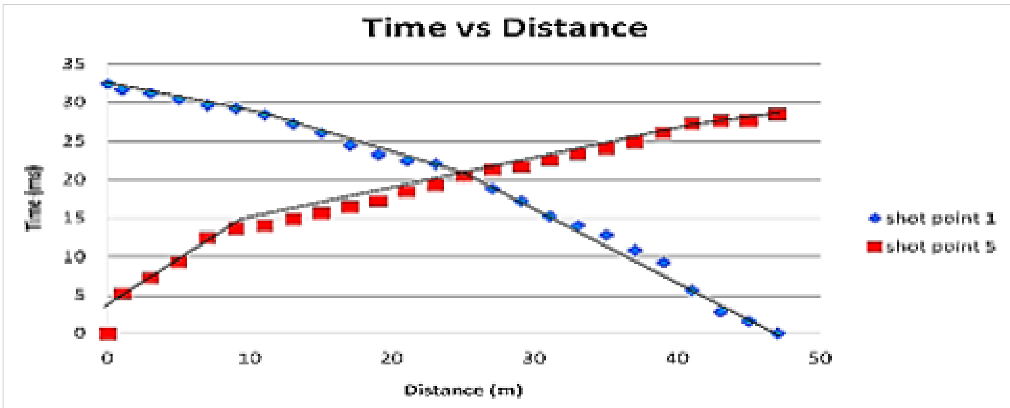

Figure 4: Travel time versus Distance plot

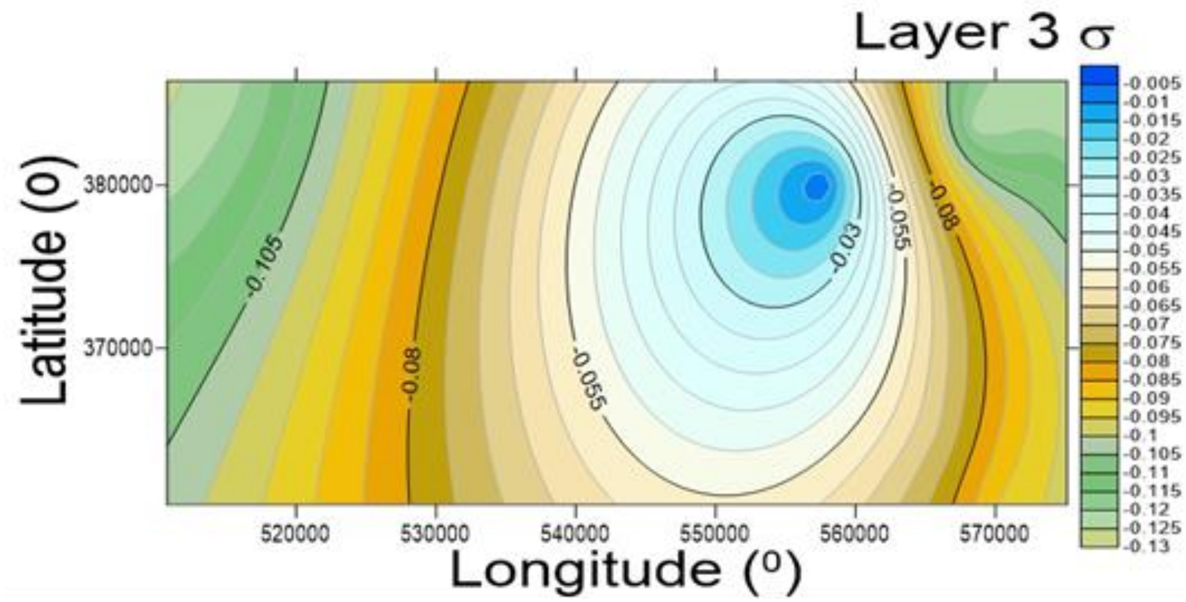

Figure 5: 2-D contour map showing the distribution of σ in layer 3

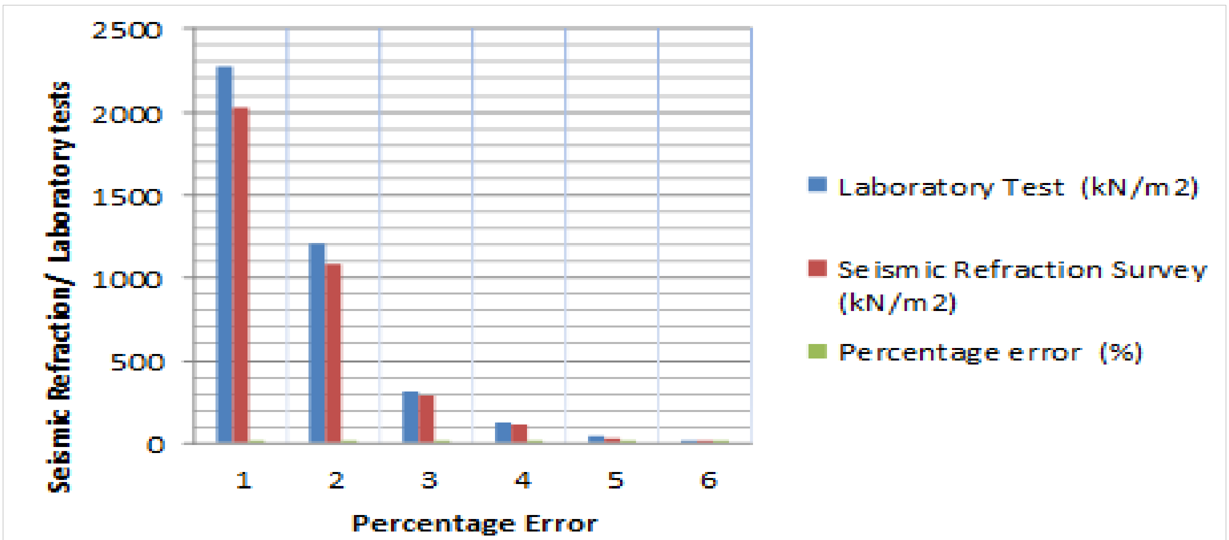

Figure 6: Seismic refraction / laboratory test and percentage error of the study area

5. Conclusion

The integration of seismic refraction and laboratory testing techniques required a broad collocate of soil parameters and slope FOS to be taken into consideration. This could be seen in its ability to identify the foundation of slope stability and aid in assembling aerial data on high hilly terrain with constraints of the study area. It is worthwhile to conclude that the advancement of slope FOS classification charts created from seismic refraction data can become an alternative for subsurface geophysicists and engineers to ascertain the slope stability of an area. This practice of seismic refraction survey preserves time, and energy, and most significantly reduces expenses for slope stability investigation. Moreover, a decrease in soil shear strength along with an increase in shear force which is the major cause of slope failure in the study area has to be adhered to. This will improve the stability of the soil by increasing its strength along with the reduction of soil mass. Futuristically, more research should be carried out as regards integrating other geophysical methods such as electrical resistivity and gravity methods, in sequence to complement our findings and identify other soil stability anomalies.

Acknowledgements

The authors are grateful to all qualified cadres during the fieldwork and the geotechnical unit, Ministry of Work, Akwa Ibom State, Nigeria for the laboratory test analysis.

References

Abudeif, A.M., Raef, A.E., Moneim, A.A., Mohammed, M.A., Farrag, A.F., 2017. Dynamic geotechnical properties Evaluation of a candidate nuclear power plant site (NPP): P-and S- waves seismic refraction technique, Northwestern Coast, Egypt. Soil Dynamics and Earthquake Engineering, 99, Pp. 124-136.

Aka, M.U., Okechukwu E.A., Johnson, C.I. and Dick, M.D., 2020. Assessing the Susceptibility of Structural Collapse using Seismic Refraction Method. Earth Sciences Malaysia, 4 (2), 140-145. DOI: http://doi.org/10.26480/esmy.02.2020.109.114

Akpan, A.E., and Okwueze, E.E., 2006. Shear Wave Observation in Seismic Refraction Prospecting. Journal of Mining and Geology, 24 (2), Pp. 1-2.

Asteris, P.G., Rizal, F.I.M., Koopialipoor, M., Roussis, P.C., Ferentinou, M., Armaghani, D.J., Gordan, B., 2022. Slope Stability Classification under Seismic Conditions Using Several Tree-Based Intelligent Techniques. Appl. Sci., 12, Pp. 1753. doi.org/ 10.3390/app12031753.

Gordan, B., Armaghani, D.J., Adnan, A.B., Rashid, A.S.A., 2016. A New Model for Determining Slope Stability Based on Seismic Motion Performance. Soil Mech. Found. Eng., 53, Pp. 344–351.

Imbua, D.L., 2013. Robbing Others to Pay Mary Slessor: Unearthly the Authentic Heroes and Heorines of the Aboilition of Twin –Killing in Calabar. African Economic History, 41: Pp. 139-158 ISSN 0145-2258 JSTOR 4386330.

Rasouli, M., and Mahyar, M., 2011. Assessment and comparison of occurring probability of rock failures based on empirical and kinematical methods," 4th National Conference on Rock Mechanics, Tehran.

Ray, A., Kumar, V., Kumar, A., Rai, R., Khandelwal, M., Singh, T.N., 2020. Stability prediction of Himalayan residual soil slope using artificial neural network. Nat. Hazards, 103, Pp. 3523–3540.

Sharma, L.K., Umrau, R.K., Singh, R., Ahmad, M., and Singh, T.N., 2017. Stability investigation of hill cut soil slopes along National highway 222 at Malshej Ghat, Maharashtra. Journal of the Geological Society of India, 89 (2), Pp. 165 -174.

Udeagha, A.U., Udofia, S.I., Jacob, D.E., 2013. Cultural and Socio-economic Perspectives of the conservation of ASanting Ibiono Sacred Forest in Akwa Ibom State, Nigeria. International Journal of Biodiversity and Conservation, 5 (11), Pp. 696 -703. DOI: 10.5897/IJBC2013.0580

Uhlemann, S., Hagedorn, S., Dashwood, B., Maurer, H., Gunn, D., Dijkstra, T., and Chambers, J., 2016. Landslide characterization using P-and S-wave seismic refraction tomography-The importance of elastic moduli. Journal of Applied Geophysics, 134, Pp. 64-76.

Xiao, D.Q., Zi, L., Cao, J., Au, S.K., and Kok-kwang, P., 2016. Three-dimensional slope reliability and risk assessment using auxiliary random finite element method. Computers and Geotechnics, 79, Pp. 146 -158.